Dear Prof. Nizkorodov,

We thank you again for handling our manuscript. All your comments have been fully addressed. Please see our point-by-point reply below. The revised MS with tracked changes is also attached after the reply letter.

1. Line 112-113: equations in PDF do not come out well; appear elevated. I find that notation is unnecessarily complicated in the equations on this page but if this is what people use in this community, it is fine.

Reply: Now the elevated equations have been

2. Line 130: End -> At the end

Reply: Corrected accordingly.

3. Line 174: "ppb" refers to par per billion by weight in solution? Atmospheric chemistry readers may confuse it with part per billion by volume, so perhaps it is best to define.

Reply: We agree that for the measurements of aerosol species and gaseous pollutants, our community prefers to use μg m^{-3} and ppb as unit, respectively, and this is not the case for cloudwater. We've defined "ppb" as you suggested in the revised MS.

4. Line 199: equation number missing

Reply: Added in the revised MS.

5. Line 259: variant -> varied

Reply: Corrected accordingly.

6. Figure 2: I would make points from your study a bit more prominent (they are hard to notice against bright colors of the rectangular regions)

Reply: Please check the revised version below

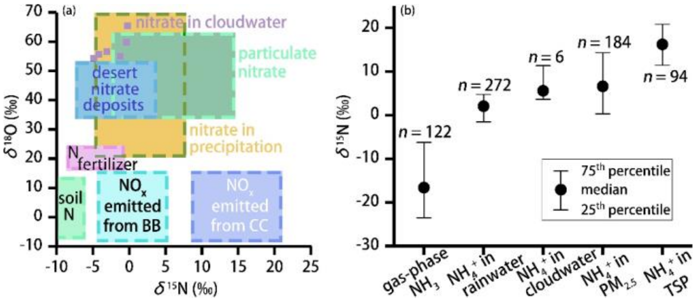

7. The supporting information file is too short to justify its existence. It only consists of one page of text, which overlaps partly with the info reported in the main text, and one Table S1. I suggest that table S1 should move to the main text and the supporting information file should be eliminated. Some people use Appendix at the end of the paper instead of supporting information section; this is also a possibility to consider.

Reply: Agree. We've moved Text S1 and Table S1 to the text as Appendix A and Appendix B, respectively.

Isotopic Constraints on the Atmospheric Sources and Formation of Nitrogenous Species in Biomass-Burning-Influenced Clouds

Yunhua Chang[1, 2], Yanlin Zhang[1*], Jiarong Li[2], Chongguo Tian[3], Linlin Song[4], Xiaoyao Zhai[1], Wenqi Zhang[1], Tong Huang[1], Yu-Chi Lin[1], Chao Zhu[2], Yunting Fang[4], Moritz F. Lehmann[5], and Jianmin Chen[2*]

[1]Yale-NUIST Center on Atmospheric Environment, Nanjing University of Information Science & Technology, Nanjing 210044, China.

[2]Shanghai Key Laboratory of Atmospheric Particle Pollution and Prevention (LAP^3), Department of Environmental Science & Engineering, Institute of Atmospheric Sciences, Fudan University, Shanghai 200433, China.

[3]Key Laboratory of Coastal Environmental Processes and Ecological Remediation, Yantai Institute of Coastal Zone Research, Chinese Academy of Sciences, Yantai 264003, China.

[4]CAS Key Laboratory of Forest Ecology and Management, Institute of Applied Ecology, Chinese Academy of Sciences, Shenyang 110016, China.

[5]Aquatic and Isotope Biogeochemistry, Department of Environmental Sciences, University of Basel, Basel 4056, Switzerland.

[*]Corresponding authors: Yanlin Zhang (dryanlinzhang@outlook.com) and Jianmin Chen (jmchen@fudan.edu.cn).

Abstract

Predicting tropospheric cloud formation and subsequent nutrient deposition relies on understanding the sources and processes affecting aerosol constituents of the atmosphere that are preserved in cloudwater. However, this challenge is difficult to address quantitatively based on the sole use of bulk chemical properties. Nitrogenous aerosols, mainly ammonium (NH_4^+) and nitrate (NO_3^-), play a particularly important role in tropospheric cloud formation. While dry and wet (mainly rainfall) deposition of NH_4^+ and NO_3^- are regularly assessed, cloudwater deposition is often underappreciated. Here we collected cloudwater samples at the summit of Mt. Tai (1545 m above sea level) in Eastern China during a long-lasting biomass burning (BB) event, and simultaneously measured for the first time the isotopic compositions (mean ± 1σ) of cloudwater nitrogen species (δ^{15}N-NH_4^+ = -6.53 ± 4.96‰, δ^{15}N-NO_3^- = -2.35 ± 2.00‰, δ^{18}O-NO_3^- = 57.80 ± 4.23‰), allowing insights into their sources and potential transformation mechanism within the clouds. Large contributions of BB to the cloudwater NH_4^+ (32.9 ± 4.6%) and NO_3^- (28.2 ± 2.7%) inventories were confirmed through a Bayesian isotopic mixing model, coupled with our newly-developed computational quantum chemistry module. Despite an overall reduction in total anthropogenic NO_x emission due to effective emission control actions and stricter emission standards for vehicles, the observed cloud δ^{15}N-NO_3^- values suggest that NO_x emissions from transportation may have exceeded emissions from coal combustion. δ^{18}O-NO_3^- values imply that the reaction of OH with NO_2 is the dominant pathway of NO_3^- formation (57 ± 11%), yet the contribution of heterogeneous hydrolysis of dinitrogen pentoxide was almost as important (43 ± 11%). Although the limited sample set used here results in a relatively large uncertainty with regards to the origin of cloud-associated nitrogen deposition, the high concentrations of inorganic nitrogen imply that clouds represent an important source of nitrogen, especially for nitrogen-

limited ecosystems in remote areas. Further simultaneous and long-term sampling of aerosol, rainfall, and cloudwater is vital for understanding the anthropogenic influence on nitrogen deposition in the study region.

1 Introduction

Nitrogenous aerosols, mainly nitrate (NO_3^-) and ammonium (NH_4^+), formed from the emissions of nitrogen oxides (NO_x = NO + NO_2) and ammonia (NH_3), are major chemical components of aerosols, which serve as cloud condensation nuclei (CCN) and thus play an important role during cloud formation in the troposphere (Gioda et al., 2011; van Pinxteren et al., 2016). Cloudwater-containing nitrogenous compounds also represent a vital contributor to nitrogen (N) budgets of terrestrial (Li et al., 2016b; Liu et al., 2013; Weathers and Likens, 1997; Vega et al., 2019) and marine ecosystems (Kim et al., 2014; Okin et al., 2011). However, the sources and formation processes of cloudwater N species are only poorly understood.

NO_x can be emitted from both anthropogenic and natural sources. Globally, over 50% of the NO_x emissions derive from combustion of fossil fuel (~ 25 Tg N yr^{-1}; Jaegle et al., 2005; Richter et al., 2005; Duncan et al., 2016), with the remainder being primarily soil-related emissions (~ 9 Tg N yr^{-1};Lamsal et al., 2011; Price et al., 1997; Yienger et al., 1995; Miyazaki et al., 2017), or deriving from biomass burning (~ 6 Tg N yr^{-1}), and lightning (2-6 Tg N yr^{-1}) (Anenberg et al., 2017; Levy et al., 1996). The atmospheric sinks of NO_x include the production of $HNO_{3(g)}$ and the formation of aerosol NO_3^- (Seinfeld and Pandis, 2012), the partitioning of which can vary with time (Morino et al., 2006). As for NH_3, over 90% of the NH_3 emissions in terrestrial ecosystems originate from agricultural production, such as livestock breeding and NH_3-based fertilizer application (Paulot et al., 2014; Kang et al., 2016; Reis et al., 2009; Bouwman et al., 1997; Heald et al., 2012; Zhang et al., 2018; Balasubramanian et al., 2015; Huang et al., 2011). In the urban atmosphere, recent studies suggest that non-agricultural activities like wastewater discharge (Zhang et al., 2017), coal burning (Li et al., 2016a), solid waste (Reche et al., 2012), on-road traffic (Suarez-Bertoa et al., 2014), and green space (Teng et al., 2017) also contribute to NH_3 emissions. In reactions with H_2SO_4 and HNO_3, NH_3 contributes to the formation of NH_4^+ salts, which typically make up from 20 to 80% of fine particle ($PM_{2.5}$) in the atmosphere (Seinfeld and Pandis, 2012).

Biomass burning (BB) is an important source of N in the atmosphere (Lobert et al., 1990; Souri et al., 2017). During the harvest/hot season of eastern China, agricultural BB frequently occurs and modifies the concentration and composition of aerosols in the atmosphere (Chen et al., 2017; Zhang and Cao, 2015). For example, about 50% of the N derived from biomass combustion can be released as NH_3 and NO_x to form particulate NH_4^+ and NO_3^-, which then account for over 80% of total nitrogenous species in BB smoke particles (Crutzen and Andreae, 1990). BB-induced aerosols have not only been associated with poor air quality and the detrimental effects on human health, they have also shown to exert manifold effects on tropospheric clouds, altering regional or even global radiation budgets (Chen et al., 2014; Norris et al., 2016; Voigt and Shaw, 2015).

The optical and chemical properties of clouds (and thus their radiative forcing) are directly related to the aerosol and precipitation chemistry (Seinfeld et al., 2016). Moreover, clouds represent reactors of multiphase chemistry, contributing to many chemical transformations that would otherwise not take place, or would proceed at much slower rates (Herrmann et al., 2015; Lance et al., 2017; Ravishankara, 1997; Schurman et al., 2018; Slade et al., 2017). Understanding the sources and fate of nitrogenous species in BB-influenced clouds is particularly important to comprehensively assess the environmental impacts of BB. But this challenge is difficult to address based on the sole use of bulk chemical properties (as most often done in previous studies).

Given that the ^{15}N can be preserved between the sources and sinks of NO$_x$ and NH$_3$, the N isotopic composition of NO$_3^-$ (δ^{15}N-NO$_3^-$) and NH$_4^+$ (δ^{15}N-NH$_4^+$) can be related to different sources of NO$_x$ and NH$_3$, and thus delivers useful information regarding the partitioning of the origins of atmospheric/cloudwater NO$_x$ and NH$_3$, respectively (Hastings et al., 2013; Michalski et al., 2005; Morin et al., 2008; Chang et al., 2018). This is different for the O isotopes. NO$_3^-$ production involves the oxidation of NO. The first step in the overall process is the conversion of NO into NO$_2$, e.g., through the oxidation by either ozone (O$_3$) or peroxy radicals (Michalski et al., 2011). Significant ^{18}O enrichments and excess ^{17}O (i.e., clear evidence for mass independent fractionation) are observed in atmospheric NO$_3^-$ collected across the globe (e.g., Michalski et al., 2005; Hastings et al., 2003). Such diagnostic isotope signatures, as well as their variability in space and time have been linked to the extent of O$_3$ oxidation (Michalski et al., 2011). Put another way, the oxygen isotope composition of NO$_3^-$ (δ^{18}O-NO$_3^-$) is largely determined by chemical reactions rather than the source, and it it is primarily modulated by the O-atom exchange (Michalski et al., 2011).in the atmosphere Therefore, δ^{18}O-NO$_3^-$ has the potential to indicate the relative importance of various NO$_3^-$ formation pathways (i.e., oxidation pathways during conversion of nitrogen oxides to NO$_3$) (Alexander et al., 2009; Elliott et al., 2009).

The O isotope fractionation during the conversion of NO$_x$ to HNO$_3$/NO$_3^-$ ($\varepsilon_{\mathrm{O}\left(\mathrm{NO_x} \leftrightarrow \mathrm{HNO_3}\right)} \big/ \varepsilon_{\mathrm{O}\left(\mathrm{NO_x} \leftrightarrow \mathrm{NO_3^-}\right)}$) involves two oxidation pathways (Hastings et al., 2003)

带格式的: 字体对齐方式: 居中

$$\begin{aligned} \varepsilon_{\mathrm{O}\left(\mathrm{NO_x} \leftrightarrow \mathrm{NO_3^-}\right)} &= \varepsilon_{\mathrm{O}\left(\mathrm{NO_x} \leftrightarrow \mathrm{HNO_3}\right)} = \gamma \times \varepsilon_{\mathrm{O}\left(\mathrm{NO_x} \leftrightarrow \mathrm{NO_3^-}\right)_{\mathrm{OH}}} + (1-\gamma) \times \varepsilon_{\mathrm{O}\left(\mathrm{NO_x} \leftrightarrow p\mathrm{NO_3^-}\right)_{\mathrm{H_2O}}} \\ &= \gamma \times \varepsilon_{\mathrm{O}\left(\mathrm{NO_x} \leftrightarrow \mathrm{HNO_3}\right)_{\mathrm{OH}}} + (1-\gamma) \times \varepsilon_{\mathrm{O}\left(\mathrm{NO_x} \leftrightarrow \mathrm{HNO_3}\right)_{\mathrm{H_2O}}} \end{aligned} \quad (1)$$

where $\gamma/(1-\gamma)$ represents the contribution ratio of the isotope fractionation associated with the formation of HNO$_3$/NO$_3^-$ through the "OH+NO$_2$" pathway ($\varepsilon_{\mathrm{O}\left(\mathrm{NO_x} \leftrightarrow \mathrm{NO_3^-}\right)_{\mathrm{OH}}}$) and the hydrolysis of dinitrogen pentoxide (N_2O_5) ($\varepsilon_{O\left(NO_x\leftrightarrow NO_3^-\right)_{H_2O}}$), respectively. The $\delta^{18}O$ value of HNO_3 produced by the former process reflects the O atom partitioning of 2/3 O_3 and 1/3 OH:

$$\begin{aligned}\varepsilon_{O\left(NO_x\leftrightarrow NO_3^-\right)_{OH}} &= \varepsilon_{O\left(NO_x\leftrightarrow HNO_3\right)_{OH}} = \frac{2}{3}\varepsilon_{O\left(NO_2\leftrightarrow HNO_3\right)_{OH}} + \frac{1}{3}\varepsilon_{O\left(NO\leftrightarrow HNO_3\right)_{OH}} \\ &= \frac{2}{3}\left[\frac{1000\left({}^{18}\alpha_{NO_2/NO}-1\right)\left(1-f_{NO_2}\right)}{\left(1-f_{NO_2}\right)+\left({}^{18}\alpha_{NO_2/NO}\times f_{NO_2}\right)}+\left(\delta^{18}\text{O-NO}_x\right)\right]+ \\ &\frac{1}{3}\left[\left(\delta^{18}\text{O-H}_2\text{O}\right)+1000\left({}^{18}\alpha_{OH/H_2O}-1\right)\right]\end{aligned} \tag{2}$$

As for the $\delta^{18}O$ value of HNO_3 formed during hydrolysis of N_2O_5, 5/6 of the O atoms is derived from O_3 and 1/6 from OH (Hastings et al., 2003):

$$\varepsilon_{O\left(NO_x\leftrightarrow NO_3^-\right)_{H_2O}} = \varepsilon_{O\left(NO_x\leftrightarrow HNO_3\right)_{H_2O}} = \frac{5}{6}\left(\delta^{18}\text{O-N}_2\text{O}_5\right)+\frac{1}{6}\left(\delta^{18}\text{O-H}_2\text{O}\right) \tag{3}$$

where f_{NO_2} refers to the fraction of NO_2 in the total NO_x pool. Values for f_{NO_2} vary between 0.2 and 0.95 (Walters and Michalski, 2015). δ^{18}O-X is the O isotopic composition of X. The range of δ^{18}O-H_2O can be approximated using an estimated tropospheric water vapor $\delta^{18}O$ range of -25‰-0‰ (Zong et al., 2017). The $\delta^{18}O$ of NO_2 and N_2O_5 varies between 90‰ and 122‰ (Zong et al., 2017). ${}^{18}\alpha_{NO_2/NO}$ and ${}^{18}\alpha_{OH/H_2O}$ represent the equilibrium O isotope fractionation factor between NO_2 and NO, and OH and H_2O, respectively, which is temperature-dependent

$$1000\left({}^{m}\alpha_{X/Y}-1\right)=\frac{A}{T^4}\times10^{10}+\frac{B}{T^3}\times10^{8}+\frac{C}{T^2}\times10^{6}+\frac{D}{T}\times10^{4} \tag{4}$$

where A, B, C, and D are experimental constants over the temperature range of 150-450 K. Based on Equations 1-4 and measured values for δ^{18}O-NO_3^- of cloudwater, a Monte Carlo simulation was performed to generate 10000 feasible solutions. The error between predicted and measured $\delta^{18}O$ was less than 0.5‰.

At the ~~E~~end of July 2015, a large-scale BB event occurred over eastern and northern China. We took advantage of this special event to collect cloudwater samples at a high-altitude mountaintop site in the North China Plain, and to calibrate the isotopic signatures that BB events leave in the N pool of clouds. Integrating cloudwater nitrogenous species isotope data ($\delta^{15}N\text{-}NH_4^+$, $\delta^{15}N\text{-}NO_3^-$ and $\delta^{18}O\text{-}NO_3^-$) in a Bayesian isotopic mixing model coupled with a newly developed computational quantum chemistry module (Chang et al., 2018), and using an isotopic mass balance approach, the sources and production pathways of inorganic nitrogen in cloudwater were quantified. Although numerous studies have been conducted that involved the chemical characterization of fog water or cloudwater, to our knowledge, there are no reports on the N (and O) isotopic composition of both NO_3^- *and* NH_4^+ in cloudwater.

2 Materials and Methods

2.1 Cloudwater Sample Collection

Mt. Tai (117°13′ E, 36°18′ N; 1545 m above sea level) is a world-recognized geopark of key natural, historical and cultural significance, located in the eastern North China Plain (Fig. 1). It belongs to China’s most important agricultural and industrial production areas, and the composition of the atmosphere near the mountain can be considered representative with regards to the quality and levels of atmospheric pollution in the region (Li et al., 2017; Liu et al., 2018). Given the opportunistic nature of this study, cloudwater sampling commenced at the summit of Mt. Tai three days after the fire began (08/01/2015 19:12 to 08/03/2015 6:12; Table 1). In total, six cloudwater samples were collected during the long-lasting cloud event using a single-stage

Caltech active strand cloud-water collector (CASCC), as described by (Demoz et al., 1996). The cloud collector was cleaned prior to each sampling using high-purity deionized water. After sampling, cloud samples were filtered immediately using disposable syringe filters (0.45 µm) to remove any suspended particulate matter, and then stored in a freezer at -80 ^{o}C until further analysis. More details on the monitoring site and sampling procedures can be found elsewhere (Li et al., 2017).

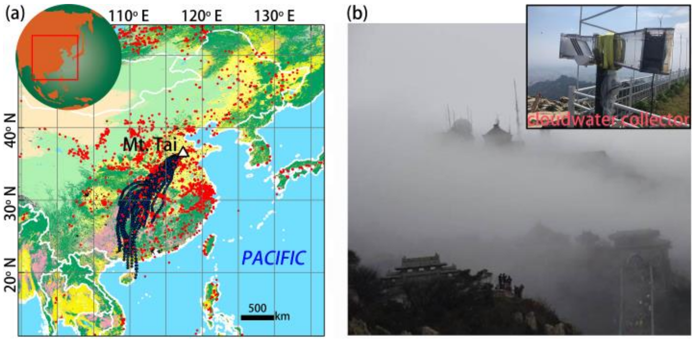

Figure 1. (**a**) Location of Mt. Tai (triangle) and twenty-four 48-h back trajectories (black lines) of air masses simulated by the HYSPLIT model (http://ready.arl.noaa.gov/HYSPLIT.php) based on the Global Data Assimilation System (GDAS) meteorological data set arriving at Mt. Tai on 1 August 2015 (4:00 UTC) at an altitude 1500-m a.s.l (close to the altitude of our sampling site). The base map of land use in China was modified from Chang et al. (2018). The red dots represent the positions of wildfires between 29 and 31 July 2015, based on moderate-resolution imaging spectroradiometer (MODIS) (http://modis-fire.umd.edu). (**b**) Field photos of clouds-shrouded Mt. Tai and the cloudwater collector.

2.2 Chemical and Isotopic Analysis

Inorganic ions (including SO_4^{2-}, NO_3^-, Cl^-, NH_4^+, K^+, Ca^{2+}, Mg^{2+}, and Na^+), as well as levoglucosan, a specific tracer of biomass burning, in cloudwater samples were analyzed using a Dionex^{TM} ICS-5000$^+$ system (ThermoFisher Scientific, Sunnyvale, USA). The IC system was equipped with an automated sampler (AS-DV). Cloudwater samples were measured using an IonPac CG12A guard column and a CS12A separation column, with an aqueous methanesulfonic acid (MSA, 30 mM L^{-1}) eluent at a flow rate of 1 mL min^{-1}. Detailed information regarding sample processing, pre-treatment, chemical analyses, and analytical protocol adaption can be found elsewhere (Cao et al., 2016, 2017). The detection limits for Na^+, NH_4^+, K^+, Mg^{2+}, Ca^{2+}, Cl^-, NO_2^-, NO_3^-, SO_4^{2-}, and levoglucosan are 0.06, 0.03, 0.12, 0.08, 0.13, 0.64, 1.11, 2.67, 1.41, and 1.29 ppb (part per billion by weight in solution), respectively. The analytical errors from duplicate analysis were within 5%.

Analysis of the isotopic compositions of NH_4^+ ($\delta^{15}N\text{-}NH_4^+$) and NO_3^-, ($\delta^{15}N\text{- }NO_3^-$ and $\delta^{18}O\text{-}NO_3^-$) was based on the isotopic analysis of nitrous oxides (N_2O) after chemical conversion of the respective target compound. More precisely, dissolved NH_4^+ in cloudwater samples was oxidized to NO_2^- by alkaline hypobromite (BrO^-), and then reduced to N_2O by hydroxylamine hydrochloride ($NH_2OH.HCl$) (Liu et al., 2014). NO_3^- was initially transformed to NO_2^- by cadmium, and then further reduced to N_2O by sodium azide (NaN_3) in an acetic acid buffer (McIlvin and Altabet, 2005; Tu et al., 2016). The produced N_2O was analyzed using a purge and cryogenic trap system (Gilson GX-271, IsoPrime Ltd., Cheadle Hulme, UK), coupled to an isotope ratio mass spectrometer (PT-IRMS) (IsoPrime 100, IsoPrime Ltd., Cheadle Hulme, UK). In order to correct for any machine drift and procedural blank contribution, international NH_4^+ (IAEA N1, USGS 25, and USGS 26) and NO_3^- (IAEA N3, USGS 32, and USGS 34) standards were processed in the same way as samples. Standard regressions were made based on the known isotopic values of international standards and the measured standard δ^{15}N values. The slope of the plot of the sample versus the standard δ^{15}N (0.49) was very close to the expected slope (0.5), which can be predicted based on the fact that half of the N atoms were derived from the azide (McIlvin and Altabet, 2005). The r^2 of the regression line was 0.999. The analytical precision for both multiple N and O isotopic analyses was better than 0.3‰ (n = 5).

2.3 Bayesian Mixing Model Analysis

By taking the uncertainty associated with the N isotopic signatures of multiple sources and associated isotope fractionation during (trans-)formations into account, the Bayesian method is more appropriate than simple linear mixing modeling to yield estimates on the source partitioning of a mixture like air pollutants (Chang et al., 2016; Chang et al., 2018). The relative contribution of each source in Bayesian theorem is expressed as:

$$P\left(f_q|data\right) = \theta\left(data\middle|f_q\right) \times P\left(f_q\right) \Big/ \sum \theta\left(data\middle|f_q\right) \times P\left(f_q\right) \quad (5)$$

带格式的: 字体对齐方式: 居中

where θ(data|f_q) and P(f_q) represent the likelihood of the given mixed isotope signature, and the pre-determined probability of the given state of nature, based on prior information, respectively. The denominator represents the numerical approximation of the marginal probability of the data. Here the Bayesian mixing model MixSIR (stable isotope mixing models using sampling-importance-resampling) was used to disentangle the various potential NH_3 and NO_x sources contributing to the cloudwater NH_4^+ and NO_3^- pools, respectively, by forming the true probability distributions through generating 10000 solutions of source apportionment. Details on the model approach can be found in Appendix A~~SI Text S1~~.

The measured δ^{15}N-NO_3^- values of cloudwater samples depend on the δ^{15}N signatures of the original NO_x sources (δ^{15}N-NO_x), the N isotope fractionation between nitrogen oxides (i.e., NO and NO_2 (Walters et al., 2016)), and the N isotope enrichment factor (ε_N) associated with the kinetic transformation of NO_x to HNO_3 (Walters and Michalski, 2015). ε_N is considered a hybrid of two dominant processes: one is the reaction of NO_2 and OH radicals to form NO_3^-, the other is the heterogeneous hydrolysis of dinitrogen pentoxide (N_2O_5) with water to form NO_3^-. We recently developed a quantum chemistry computation module to quantify the N fractionation during nitrate formation, which had been validated by field measurements (Chang et al., 2018). Here this module was adopted to calculate the N isotope fractionation during NO_3^- formation, and in turn to correct the raw δ^{15}N-NO_3^- values of cloudwater samples.

While the N isotopic source signatures of NO_x are relatively well constrained (Table ~~S1~~B1 in Appendix B), this is not the case for NH_3. We recently established a pool of isotopic source signatures of NH_3 in eastern China, in which livestock breeding and fertilizer application were identified to produce NH_3 with a δ^{15}N of -29.1 ± 1.7‰ and -50.0 ± 1.8‰, respectively (Chang et al., 2016). Although fossil-fuel combustion, urban waste, and natural soils also represent potential sources of NH_3, their impacts are probably minor compared to that of agricultural and biomass burning emissions, at least on a regional (or greater) scale (Kang et al., 2016). For the N isotope signature of biomass burning-derived NH_3 we assumed 12‰ (Kawashima and Kurahashi, 2011), a value that has also been applied in other recent isotope-based source apportionment studies (e.g., Chellman et al., 2016; Wang et al., 2017a).

3 Results and Discussion

3.1 Chemical characterization of biomass-burning-influenced clouds

The moderate-resolution imaging spectroradiometer (MODIS) wildfire map (Fig. 1) shows that there were intensive biomass burning events occurring over mainland China, end of July 2015, just before the study period. Moreover, analysis of the back trajectories of air masses at the study site revealed the strong influence by atmospheric transport from regions that also experienced intensive biomass burning events shortly before the sampling campaign. It can thus be assumed that large amounts of BB-related pollutants were transported from the southwest to the sampling site at Mt. Tai. Table 1 compiles sample information and results from the chemical and isotopic analysis of cloudwater samples in this study. The concentrations of NO_3^- and NH_4^+ ranged from 4.9 to 19.9 mg L^{-1} (10.1 mg L^{-1} on average), and from 4.9 to 18.0 mg L^{-1} (9.1 mg L^{-1} on average), respectively, much higher than during non-BB seasons (Chen et al., 2017; Desyaterik et al., 2013; Li et al., 2017, 2018; Lin et al., 2017). Similarly, levoglucosan in our cloudwater samples varied between 12.1 and 35.1 μg L^{-1} (19.9 μg L^{-1} on average), and concentrations were thus one order of magnitude higher than those documented during non-BB seasons (Boone et al., 2015; Fomba et al., 2015). Although levoglucosan can be oxidized by OH radicals in the tropospheric aqueous phase (Sang et al., 2016), it is nevertheless a reliable marker compound for BB due to its high emission factors and relatively high concentrations in the ambient aerosols (Hoffmann et al., 2010). In our study, the concentrations of NO_3^- ($r^2 = 0.55$) and NH_4^+ ($r^2 = 0.66$) are strongly correlated with that of levoglucosan, suggesting that the pronounced increase of NO_3^- and NH_4^+ levels observed here can at least be partly attributed to BB activities during the study period. Globally, BB accounts for around 10% of NH_3 and NO_x emissions (Benkovitz et al., 1996; Bouwman et al., 1997; Olivier et al., 1998; Schlesinger and Hartley, 1992).

Table 1. Sampling details and results of chemical and isotopic analysis for collected cloudwater samples.

Date	Local time	NO_3^- (mg L^{-1})	NH_4^+ (mg L^{-1})	levoglucosan (µg L^{-1})	$\delta^{15}N$-NO_3^- (‰)	$\delta^{18}O$-NO_3^- (‰)	$\delta^{15}N$-NH_4^+ (‰)
Aug 1	19:12-22:58	19.86	17.99	35.06	-0.22	65.46	3.62
	23:45-08:25	4.88	4.92	12.11	-1.28	55.01	3.85
Aug 2	09:10-12:19	5.57	5.81	23.60	-0.40	59.84	0.05
	12:55-18:30	13.24	11.51	18.67	-4.18	55.66	11.34
	20:02-23:06	10.06	7.74	13.63	-3.11	56.63	12.99
	23:48-06:12	6.71	6.59	16.42	-4.92	54.19	7.33

3.2 Isotopic characterization of biomass-burning-influenced clouds

The N (and O) isotopic composition of cloudwater nitrogenous species was more (NH_4^+) or less (NO_3^-) ~~variant~~ varied (Table 1), with the average $\delta^{15}N$ values of 6.53‰ and -2.35‰ for NH_4^+ and NO_3^-, respectively. The average $\delta^{18}O$-NO_3^- value was 57.80‰. These values are generally different from gas, rainwater, and aerosol values measured worldwide (Fig. 2). Various atmospheric processes can influence the isotopic composition of atmospheric nitrogenous species including: the original emission source of NO_x, seasonality of oxidation pathways, isotope fractionation during transport, partitioning between wet and dry components, and spatial gradients in atmospheric chemistry (Elliott et al., 2007; Hastings et al., 2003). These aspects may affect the $\delta^{15}N$ and $\delta^{18}O$ values differentially. For example, the $\delta^{15}N$ of atmospheric NO_3^- retains spatial changes in the original NO_x signature quite well, in contrast to the $\delta^{18}O$. On the other hand, the $\delta^{18}O$ most strongly depends on the oxidation chemistry and formation pathway in the atmosphere (see Equations 1-4).

At present, there are no other reports on the isotope ratios of both NO_3^- and NH_4^+ in cloudwater, and a comparison is possible only with isotope data from precipitation and aerosol N. Recently, Vega et al. (2019) reported the $\delta^{15}N$ (-8‰ ± 2‰) and $\delta^{18}O$ (71‰ ± 3‰) values of NO_3^- in fog water at a forest site in Sweden. The relatively high $\delta^{15}N$ values in our study (-2.35‰) suggest more NO_x that emitted from combustion processes. In contrast, the much higher $\delta^{18}O$ values in Vega et al. (2019) indicate a much greater contribution from O_3 in sub-Arctic environments. In Fig. 2a, N isotopic differences for NO_x sources are greater (35‰), than for $\delta^{18}O$-NO_x. In fact, the oxygen isotope signature of NO_x is mainly chemistry-driven rather than determined by the source (see discussion below), and thus, $\delta^{18}O$ measurements cannot be used to address the uncertainty of the NO_x sources that may remain when just looking at $\delta^{15}N$ values alone. As shown in Fig. 2b, the $\delta^{15}N$ values of aerosol NH_4^+ are systematically higher than that of NH_3. Significant ε_N during the conversion of gas to aerosol (up to 33‰) has been proposed to alter the $\delta^{15}N$ values during the transformation of the source (NH_3) to the sink (particulate NH_4^+). Indeed, our compilation of previous results (Fig. 2b) reveals that particulate NH_4^+ (particularly in the coarse aerosol fraction) is more enriched in ^{15}N than NH_3 (by > 23‰ on average), as well as NH_4^+ in precipitation (by 18‰ on average). This can most likely be attributed to the preferential absorption ^{14}N-NH_3 associated with washout processes during precipitation (Zheng et al., 2018). We are aware of the fact that our sample/data set used here is limited, resulting in a relatively large uncertainty with regards to the N isotope-based source apportionment. However, all $\delta^{15}N$-NH_4^+ values in cloudwater samples fall within the observed range of $\delta^{15}N$-NH_4^+ values for fine particles ($PM_{2.5}$), providing putative evidence that NH_4^+ in cloudwater is primarily derived from particulate NH_4^+ rather than NH_3 absorption.

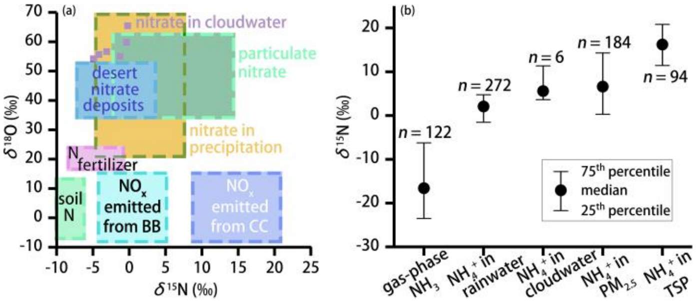

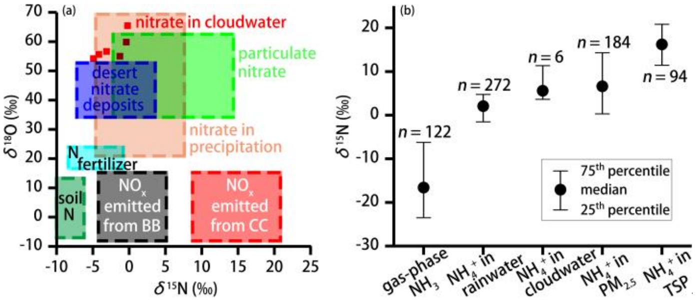

Figure 2. (**a**) Observed range of typical δ^{18}O and δ^{15}N values of NO_3^- and NO_x for different sources (adapted from Fenech et al. (2012)). BB and CC represent biomass burning and coal combustion, respectively. The red squares represent nitrate isotope data in cloudwater (this study). (**b**) The 25th percentiles, median and 75th percentiles for the δ^{15}N values of the ambient NH_3 (Chang et al., 2016; Felix et al., 2013; Savard et al., 2018; Smirnoff et al., 2012) and NH_4^+ in precipitation (Fang et al., 2011; Leng et al., 2018; Yang et al., 2014; Zhang et al., 2008), cloudwater (this study), $PM_{2.5}$ (particulate matter with aerodynamic diameter less than 2.5 μm; (Lin et al., 2016; Park et al., 2018; Proemse et al., 2012; Smirnoff et al., 2012), and TSP (particulate matter with aerodynamic diameter less than 100 μm (Kundu et al., 2010; Savard et al., 2018; Yeatman et al., 2001) are shown.

3.3 Isotope-based assessment of the sources and formation of nitrogenous species in clouds

Using the MixSIR model, the relative contribution of four NH_3 sources to NH_4^+ can be calculated, based on the isotope data of ambient $\delta^{15}N\text{-}NH_4^+$, and considering the N fractionation and prior information on the site. As upper limit for the N isotope enrichment factor associated with the conversion of NH_3 to NH_4^+ ($\varepsilon_{NH_4^+-NH_3}$), we assumed 33‰ when using MixSIR, but also considered lower values for $\varepsilon_{NH_4^+-NH_3}$ (Fig. 3a) (given the conflicting evidence with regards to $\varepsilon_{NH_4^+-NH_3}$; e.g., Deng et al., 2018; Li et al., 2012). Dependent of the choice for $\varepsilon_{NH_4^+-NH_3}$ (between 0‰ to 33‰ proposed by Heaton et al. (1997)) the relative contribution of biomass burning, fertilizer application, and livestock breeding to NH_4^+ in cloudwater ranges from 25.9% to 85.4%, 5.9% to 37.0%, and 8.7% to 85.4%, respectively. Irrespective of the uncertainty related to $\varepsilon_{NH_4^+-NH_3}$, the measurement of levoglucosan provides compelling evidence that biomass burning represents an important NH_3 source, independently validating our isotope approach. Our sampling site was located in the North China Plain, also known as the granary of China. Although non-agricultural NH_3 emissions like on-road traffic are important in the urban atmosphere (Chang et al., 2016), their contribution must be considered insignificant with respect to fertilizer application and livestock breeding in this region (Kang et al., 2016). Besides, coal-based heating in China is suspended during summertime, and coal combustion has been demonstrated to be a minor contributor of total NH_3 emissions (Li et al., 2016a). Hence the partitioning between the three main NH_3 sources appears plausible. Moreover, existing emission inventory data confirm that the ratio of NH_3 emissions in North China Plain from livestock breeding (1658 kt) and fertilizer application (1413 kt) was 1.17 (Zhang et al., 2010), which is very close to our estimate (between 0.98 and 1.14) when $\varepsilon_{NH_4^+-NH_3} \geq 25‰$. For a $\varepsilon_{NH_4^+-NH_3}$ range that we consider most plausible (i.e. between 25‰ and 33‰), the relative cloudwater NH_4^+ source partitioning between biomass burning, fertilizer application, and livestock is 32.9 ± 4.6%, 32.9 ± 3.0%, and 34.2 ± 1.6%, respectively (indicated as red square in Fig. 3a). It is important to note that there was large uncertainty in the evaluation of biomass burning, which was partly ascribed to the lack of localized isotopic source signatures in China. In addition, the isotopic fractionation from the conversion of NH_3 to NH_4^+ was simplified in this study, and it was not possible to incorporate all of the possible equilibrium and kinetic fractionation scenarios.

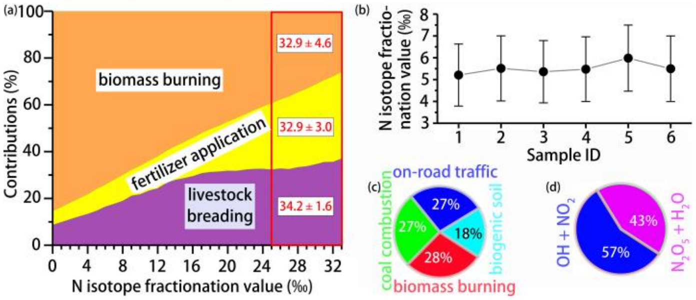

Figure 3. (**a**) Source partitioning estimates for NH_4^+ in cloudwater as a function of $\varepsilon_{NH_3\rightarrow NH_4^+}$. The red square highlights the best-guess estimates based on $\varepsilon_{NH_4^+-NH_3} \geq 25‰$). (**b**) Whisker plot of the N fractionation for the conversation of NO_x to NO_3^- ($\varepsilon_{NO_3^--NO_x}$) calculated by the computational quantum chemistry (CQC) module. The upper line, dot, and bottom line indicate the 25th percentile, median, and 75th percentile, respectively. Refer to Table 1 for sample ID. (**c**) Overall contribution of various NO_x sources to NO_3^- in cloudwater as estimated by the MixSIR model. (**d**) Overall contribution of the two dominant pathways to NO_3^- formation in cloudwater, as estimated by the MixSIR model.

The computational quantum chemistry (CQC) module in MixSIR has been proven a robust tool to quantify the N isotope enrichment factor during NO_x-NO_3^- conversion ($\varepsilon_{NO_3^--NO_x}$) (e.g., Zong et al., 2017, Chang et al., 2018). Cloudwater sample-based data from this study reveal that $\varepsilon_{NO_3^- - NO_x}$ values fall into a small range (5.21‰ to 5.98‰) (Fig. 3b), suggesting robust isotope effects during the N isotopic exchange reactions. Knowing $\varepsilon_{NO_3^- - NO_x}$, the overall contribution of various NO_x sources to NO_3^- in cloudwater can be estimated (Fig. 3c). As was expected, biomass burning was the largest contributor (28.2 ± 2.7%), followed by on-road traffic (27.1 ± 2.2%), coal combustion (26.8 ± 3.4%), and biogenic soil (17.9 ± 3.9%). The fundamental importance of biomass burning-emitted NO_x to NO_3^- in cloudwater is supported by the observed correlation between the concentrations of levoglucosan and biomass burning-derived NO_3^- ($r^2 = 0.66$). The average contribution ratio of coal combustion and on-road transportation to NO_x emissions in our study (0.99) is slightly lower than that calculated from regional emission inventories (9.0 Tg/7.4 Tg = 1.22) (Zhao et al., 2013). The apparent difference is likely real, and reflects the fact that NO_x emissions by anthropogenic activities changed significantly since 2010: a 17% total emission decrease between 2010 and 2017 can primarily be attributed to upgraded emission standards and new “ultra-low emission” techniques in the coal-fired power plant sector, given that traffic-emitted NO_x likely increased as a consequence of the continuous expansion of auto trade market during the last decade (Chang et al., 2018). In turn, our source partitioning estimate probably reflects the most updated status of NO_x emissions in China, where transportation-related NO_x emissions have reached levels that are comparable to NO_x emissions by coal combustion. In this regard, our study demonstrates that Bayesian-based isotopic mixing modeling can be an effective and timely approach to track rapid emissions changes of NO_x in a fast-developing country like China.

Using the measured $\delta^{18}O$ and equations 1-4 (and the assumptions above), we can calculate γ, and the relative importance of the two oxidation pathways of NO_3^- formation (Fig. 3d). On average, 57% NO_3^- formation can be attributed to the “NO_2 + OH” pathway, and 43% to the “N_2O_5

+ H_2O” pathway. In the low-latitude regions, where atmospheric OH concentrations are highest, particulate NO_3^- production via the “NO_2 + OH” pathway predominates (up to 87%) (Alexander et al., 2009). Sampling during summertime, oxidation of NO_2 through OH was expected to be the dominant pathway of nitrate formation, in accordance with observations from the subtropics (Hastings et al., 2003). However, our results highlight that N_2O_5 hydrolysis can be an almost equally important process as the oxidization of NO_2 with OH with regards to the NO_3^- formation in cloudwater (Wang et al., 2017b).

4 Conclusions

In this study, we measured the isotopic composition of nitrogenous species in cloudwater at the summit of Mt. Tai during a long-lasting biomass burning event, in order to investigate the sources and processes involved in cloudwater NO_3^-/NH_4^+ formation, and in turn to test our isotope-balance approach to constrain N source partitioning in cloudwater. Using a Bayesian isotope mixing model, the δ^{15}N-based estimates confirm that at least transiently biomass burning related NH_3 and NO_x emissions is a major source of cloudwater N. Moreover, our data are in accordance with regional emission inventories for both NH_3 and NO_x, validating the Bayesian isotope mixing model approach. Based on cloud water nitrate δ^{18}O measurements, the reaction of NO_2 with OH turned out to be the dominant pathway to form cloud nitrate, yet the contribution from the heterogeneous hydrolysis of N_2O_5 to NO_3^- is almost equally important. Our study underscores the value of cloud-water dissolved inorganic nitrogen isotopes as carrier of quantitative information on regional NO_x emissions. It sheds light on the origin and production pathways of nitrogenous species in clouds and emphasizes the importance of BB-derived nitrogenous species as cloud condensation nuclei in China’s troposphere. Moreover, it highlights the rapid evolution of NO_x emissions in China. Despite an overall reduction in total anthropogenic NO_x emission due to effective emission control actions and stricter emission standards for vehicles, the relative contribution of transportation to total NO_x emissions has increased over the last decade and may already have exceeded emissions from the power sector.

Appendix A: Bayesian isotopic mixing model

带格式的: Heading-Main

设置了格式: 字体: 非加粗

The Bayesian mixing model makes use of stable isotope data to determine the probability distribution of source contributions to a mixture, explicitly accounting for uncertainties associated with multiple sources, their isotopic signatures, and isotope fractionation during transformations. The model has been widely used in ecological studies, such as food-web analyses. In Bayesian theorem, the contribution of each source is calculated based on mixed data and prior information, such that:

$$P (f_q | data) = \theta(data | f_q) \times p (f_q) / \sum\theta(data | f_q) \times p (f_q)$$

where $\theta(data|f_q)$ and $p(f_q)$ refer to the likelihood of the given mixed isotope signature, and the pre-determined probability of the given state of nature, based on prior information, respectively. The denominator represents the numerical approximation of the marginal probability of the data. In a Bayesian model (stable isotope in R; SIAR), isotope signatures from the mixed data pool are assumed to be normally distributed. Uncertainty in the distribution of isotope sources and associated isotope fractionation during transformations are factored into the model by defining respective mean (μ) and standard deviation (σ) parameters. Prior knowledge about proportional source contributions (f_q) is parametrized using the Dirichlet distribution, with an interval of [0, 1]. To assess the likelihood of the given f_q, the proposed proportional contribution is combined with a user-specified isotope distribution of sources and their associated isotope effects to develop a proposed isotope distribution for the mixture. The probability of fractional source contributions (f_q) is calculated by the Hilborn sampling-importance-resampling method.

Appendix B: Isotopic signatures of NOx emitted from various sources

带格式的: Heading-Main

设置了格式: 字体: 非加粗

Table B1. Typical δ^{15}N-NO$_x$ values for coal combustion, transportation and biomass burning, and soils based on literature values.

Source types	Mean (‰)	Standard(‰)	Number	Reference
Coal combustion	13.72	4.57	47	Felix et al., 2012, 2015
Transportation	-7.25	7.80	151	Walter et al., 2015a, b; Heaton et al., 1997
Biomass burning	1.04	4.13	24	Fibiger and Hastings, 2016; Felix and Elliott, 2013
Biogenic soil	-33.77	12.16	6	Hastings et al., 2009; Felix et al., 2012

Data availability

All data used to support the conclusion are presented in this paper. Additional data are available upon request. Please contact the corresponding authors (Yanlin Zhang (dryanlinzhang@outlook.com) and Jianmin Chen (jmchen@fudan.edu.cn)).

Acknowledgments

This study was supported by the National Key R&D Program of China (Grant no. 2017YFC0212700, task 1 and 4), National Natural Science Foundation of China (Grant nos. 41975166, 41705100, 91644103), the Provincial Natural Science Foundation of Jiangsu (Grant nos. BK20180040, BK20170946), University Science Research Project of Jiangsu Province (17KJB170011), the University of Basel research funds, the Priority Academic Program Development of Jiangsu Higher Education Institutions (PAPD), the Program for Changjiang Scholars and Innovative Research Team in University of Ministry of Education of China (PCSIRT), and the Opening Project of Shanghai Key Laboratory of Atmospheric Particle Pollution and Prevention (LAP^3).

References

Alexander, B., Hastings, M. G., Allman, D. J., Dachs, J., Thornton, J. A., and Kunasek, S. A.: Quantifying atmospheric nitrate formation pathways based on a global model of the oxygen isotopic composition ($\Delta^{17}O$) of atmospheric nitrate, Atmos. Chem. Phys., 9, 5043-5056, https://doi.org/10.5194/acp-9-5043-2009, 2009.

Anenberg, S. C., Miller, J., Minjares, R., Du, L., Henze, D. K., Lacey, F., Malley, C. S., Emberson, L., Franco, V., Klimont, Z., Heyes, C.: Impacts and mitigation of excess diesel-related NO_x emissions in 11 major vehicle markets. Nature, 545, 467-471, 2017.

Balasubramanian, S., Koloutsou-Vakakis, S., McFarland, D. M., Rood, M. J.: Reconsidering emissions of ammonia from chemical fertilizer usage in Midwest USA, J. Geophys. Res., 120, 6232-6246, 2015.

Benkovitz, C. M., Scholtz M. T., Pacyna J., Tarrasón L., Dignon J., Voldner E. C., Spiro P. A., Logan J. A., and Graedel T. E.: Global gridded inventories of anthropogenic emissions of sulfur and nitrogen, J. Geophys. Res., 101, 29239-29253, https://doi.org/10.1029/96JD00126, 1996.

Boone, E. J., Laskin, A., Laskin, J., Wirth, C., Shepson, P. B., Stirm, B. H., and Pratt, K. A.: Aqueous processing of atmospheric organic particles in cloud water collected via aircraft sampling, Environ. Sci. Technol., 49, 8523-8530, https://doi.org/10.1021/acs.est.5b01639, 2015.

Bouwman, A., Lee, D., Asman, W., Dentener, F., Van Der Hoek, K., and Olivier, J.: A global high-resolution emission inventory for ammonia, Global Biogeochem. Cy., 11, 561-587, https://doi.org/10.1029/97GB02266, 1997.

Cao, F., Zhang, S. C., Kawamura, K., and Zhang, Y. L.: Inorganic markers, carbonaceous components and stable carbon isotope from biomass burning aerosols in Northeast China, Sci. Total Environ., 572, 1244-1251, https://doi.org/10.1016/j.scitotenv.2015.09.099, 2016, 2016.

Cao, F., Zhang, S. C., Kawamura, K., Liu, X., Yang, C., Xu, Z., Fan, M., Zhang, W., Bao, M., Chang, Y., Song, W., Liu, S., Lee, X., Li, J., Zhang, G., and Zhang, Y. L.: Chemical characteristics of dicarboxylic acids and related organic compounds in $PM_{2.5}$ during biomass-burning and non-biomass-burning seasons at a rural site of Northeast China, Environ. Pollut., 231, 654-662, https://doi.org/10.1016/j.envpol.2017.08.045, 2017.

Chang, Y. H., Liu, X., Deng, C., Dore, A. J., and Zhuang, G.: Source apportionment of atmospheric ammonia before, during, and after the 2014 APEC summit in Beijing using stable nitrogen isotope signatures, Atmos. Chem. Phys., 16, 11635-11647, https://doi.org/10.5194/acp-16-11635-2016, 2016.

Chang, Y. H., Zhang, Y., Tian, C., Zhang, S., Ma, X., Cao, F., Liu, X., Zhang, W., Kuhn, T., and Lehmann, M. F.: Nitrogen isotope fractionation during gas-to-particle conversion of NO_x to NO_3^- in the atmosphere - implications for isotope-based NO_x source apportionment, Atmos. Chem. Phys., 18, 11647-11661, https://doi.org/10.5194/acp-18-11647-2018, 2018.

Chellman, N. J., Hastings, M. G., and McConnell, J. R.: Increased nitrate and decreased $\delta^{15}N$-NO_3^- in the Greenland Arctic after 1940 attributed to North American oil burning, Cryosphere Discus, https://doi.org/10.5194/tc-2016-163, 2016.

Chen, J. M., Li, C., Ristovski, Z., Milic, A., Gu, Y., Islam, M. S., Wang, S., Hao, J., Zhang, H., He, C., Guo, H., Fu, H., Miljevic, B., Morawska, L., Thai, P., Lam, Y. F., Pereira, G., Ding, A., Huang, X., and Dumka, U. C.: A review of biomass burning: Emissions and impacts on air quality, health and climate in China, Sci. Total Environ., 579, 1000-1034, https://doi.org/10.1016/j.scitotenv.2016.11.025, 2017.

Chen, Y. C., Christensen, M. W., Stephens, G. L., and Seinfeld, J. H.: Satellite-based estimate of global aerosol-cloud radiative forcing by marine warm clouds, Nature Geosci., 7, 643, https://doi.org/10.1038/ngeo2214, 2014.

Crutzen, P. J., and Andreae, M. O.: Biomass burning in the tropics: Impact on atmospheric chemistry and biogeochemical cycles. Science, 250(4988), 1669-1678, https://doi.org/10.1126/science.250.4988.1669, 1990.

Demoz, B. B., Collett, J. L., and Daube, B. C.: On the Caltech active strand cloudwater collectors, Atmos. Res., 41, 47-62, https://doi.org/10.1016/0169-8095(95)00044-5, 1996.

Deng, Y., Li, Y., and Li, L.: Experimental investigation of nitrogen isotopic effects associated with ammonia degassing at 0-70 °C, Geochim. Cosmochim. Ac., 226, 182-191, https://doi.org/10.1016/j.gca.2018.02.007, 2018.

Desyaterik, Y., Sun, Y., Shen, X., Lee, T., Wang, X., Wang, T., and Collett, J. L.: Speciation of "brown" carbon in cloud water impacted by agricultural biomass burning in eastern China, J. Geophys. Res., 118, 7389-7399, https://doi.org/10.1002/jgrd.50561, 2013.

Duncan, B. N., Lamsal, L. N., Thompson, A. M., Yoshida, Y., Lu, Z., Streets, D. G., Hurwitz, M. M., Pickering, K. E.: A space-based, high-resolution view of notable changes in urban NO_x pollution around the world (2005-2014), J. Geophys. Res., 121, 976-996, 2016.

Elliott, E., Kendall, C., Wankel, S. D., Burns, D., Boyer, E., Harlin, K., Bain, D., and Butler, T.: Nitrogen isotopes as indicators of NO_x source contributions to atmospheric nitrate deposition across the Midwestern and northeastern United States, Environ. Sci. Technol., 41, 7661-7667, https://doi.org/10.1021/es070898t, 2007.

Elliott, E. M., Kendall, C., Boyer, E. W., Burns, D. A., Lear, G. G., Golden, H. E., Harlin, K., Bytnerowicz, A., Butler, T. J., and Glatz, R.: Dual nitrate isotopes in dry deposition: Utility for partitioning NO_x source contributions to landscape nitrogen deposition, J. Geophys. Res., 114, https://doi.org/10.1029/2008jg000889, 2009.

Fang, Y. T., Koba, K., Wang, X. M., Wen, D. Z., Li, J., Takebayashi, Y., Liu, X. Y., and Yoh, M.: Anthropogenic imprints on nitrogen and oxygen isotopic composition of precipitation nitrate in a nitrogen-polluted city in southern China, Atmos. Chem. Phys., 11, 1313-1325, https://doi.org/10.5194/acp-11-1313-2011, 2011.

Fibiger, D. L., and Hastings, M. G.: First measurements of the nitrogen isotopic composition of NO_x from biomass burning, Environ. Sci. Technol., 50, 11569-11574, https://doi.org/10.1021/acs.est.6b03510, 2016.

Felix J. D., and E. M. Elliott.: The agricultural history of human-nitrogen interactions as recorded in ice core δ^{15}N-NO_3^-, Geophys. Res. Lett., 40, 1642-1646, https://doi.org/10.1002/grl.50209, 2013.

设置了格式: 下标

Felix, J. D., and Elliott, E. M.: Isotopic composition of passively collected nitrogen dioxide emissions: Vehicle, soil and livestock source signatures, Atmos. Environ., 92, 359-366, https://doi.org/10.1016/j.atmosenv.2014.04.005, 2014.

Felix, J. D., Elliott, E. M., Avery, G. B., Kieber, R. J., Mead, R. N., Willey, J. D., and Mullaugh, K. M.: Isotopic composition of nitrate in sequential Hurricane Irene precipitation samples: Implications for changing NO_x sources, Atmos. Environ., 106, 191-195, https://doi.org/10.1016/j.atmosenv.2015.01.075, 2015.

Felix, J. D., Elliott, E. M., Gish, T. J., McConnell, L. L., and Shaw, S. L.: Characterizing the isotopic composition of atmospheric ammonia emission sources using passive samplers and a combined oxidation-bacterial denitrifier approach, Rapid Commun. Mass Sp., 27, 2239-2246, https://doi.org/10.1002/rcm.6679, 2013.

Felix, J. D., Elliott, E. M., and Shaw, S. L.: Nitrogen isotopic composition of coal-fired power plant NO_x: Influence of emission controls and implications for global emission inventories, Environ. Sci. Technol., 46, 3528-3535, https://doi.org/10.1021/es203355v, 2012.

Fenech, C., Rock, L., Nolan, K., Tobin, J., and Morrissey, A.: The potential for a suite of isotope and chemical markers to differentiate sources of nitrate contamination: a review. Water Res., 46, 2023-2041, https://doi.org/10.1016/j.watres.2012.01.044, 2012.

Fibiger, D. L., and Hastings, M. G.: First measurements of the nitrogen isotopic composition of NO_x from biomass burning, Environ. Sci. Technol., 50, 11569-11574. 10.1021/acs.est.6b03510, 2016.

Fomba, K. W., van Pinxteren, D., Müller, K., Iinuma, Y., Lee, T., Collett, J. L., and Herrmann, H.: Trace metal characterization of aerosol particles and cloud water during HCCT 2010, Atmos. Chem. Phys., 15, 8751-8765, https://doi.org/10.5194/acp-15-8751-2015, 2015.

Gioda, A., Reyes-Rodríguez, G. J., Santos-Figueroa, G., Collett, J. L., Decesari, S., Ramos, M. d. C. K. V., Bezerra Netto, H. J. C., de Aquino Neto, F. R., and Mayol-Bracero, O. L.: Speciation of water-soluble inorganic, organic, and total nitrogen in a background marine environment: Cloud water, rainwater, and aerosol particles, J. Geophys. Res., 116, https://doi.org/10.1029/2010JD015010, 2011.

Hastings, M., Casciotti, K. L., and Elliott, E. M.: Stable isotopes as tracers of anthropogenic nitrogen sources, deposition, and impacts. Elements, 9, 339-344, https://doi.org/10.2113/gselements.9.5.339, 2013.

Hastings, M., Jarvis, J., and Steig, E.: Anthropogenic impacts on nitrogen isotopes of ice-core nitrate. Science, 324, 1288, https://doi.org/10.1126/science.1170510, 2009.

Hastings, M., Sigman, D. M., and Lipschultz, F.: Isotopic evidence for source changes of nitrate in rain at Bermuda, J. Geophys. Res., 108, https://doi.org/10.1029/2003JD003789, 2003.

Heald, C. L., Collett Jr, J., Lee, T., Benedict, K., Schwandner, F., Li, Y., Clarisse, L., Hurtmans, D., Van Damme, M., Clerbaux, C.: Atmospheric ammonia and particulate inorganic nitrogen over the United States, Atmos. Chem. Phys., 12(21), 10295-10312, 2012.

Heaton, T. H. E., Spiro, B., and Robertson, S. M. C.: Potential canopy influences on the isotopic composition of nitrogen and sulphur in atmospheric deposition. Oecologia, 109, 600-607, https://doi.org/10.1007/s004420050122, 1997.

Herrmann, H., Schaefer, T., Tilgner, A., Styler, S. A., Weller, C., Teich, M., and Otto, T.: Tropospheric aqueous-phase chemistry: Kinetics, mechanisms, and its coupling to a changing gas phase. Chem. Reviews, 115, 4259-4334, https://doi.org/10.1021/cr500447k, 2015.

Hoffmann, D., Tilgner, A., Iinuma, Y., and Herrmann, H.: Atmospheric stability of levoglucosan: A detailed laboratory and modeling study, Environ. Sci. Technol., 44, 694-699, https://doi.org/10.1021/es902476f, 2010.

Huang, C., Chen, C. H., Li, L., Cheng, Z., Wang, H. L., Huang, H. Y., Streets, D. G., Wang, Y. J., Zhang, G. F., Chen, Y. R.: Emission inventory of anthropogenic air pollutants and VOC species in the Yangtze River Delta region, China, Atmos. Chem. Phys., 11, 4105-4120, 2011.

Jaegle, L., Steinberger, L., Martin, R. V., Chance, K.: Global partitioning of NO_x sources using satellite observations: Relative roles of fossil fuel combustion, biomass burning and soil emissions. Faraday Discus., 130, 407-423, 2005.

Kang, Y., Liu, M., Song, Y., Huang, X., Yao, H., Cai, X., Zhang, H., Kang, L., Liu, X., Yan, X., He, H., Zhang, Q., Shao, M., and Zhu, T.: High-resolution ammonia emissions inventories in China from 1980 to 2012, Atmos. Chem. Phys., 16, 2043-2058, https://doi.org/10.5194/acp-16-2043-2016, 2016.

Kawashima, H., and Kurahashi, T.: Inorganic ion and nitrogen isotopic compositions of atmospheric aerosols at Yurihonjo, Japan: Implications for nitrogen sources, Atmos. Environ., 45, 6309-6316, https://doi.org/10.1016/j.atmosenv.2011.08.057, 2011.

Kim, I. N., Lee, K., Gruber, N., Karl, D. M., Bullister, J. L., Yang, S., and Kim, T. W.: Increasing anthropogenic nitrogen in the North Pacific Ocean. Science, 346, 1102-1106, https://doi.org/10.1126/science.1258396, 2014.

Kundu, S., Kawamura, K., and Lee, M.: Seasonal variation of the concentrations of nitrogenous species and their nitrogen isotopic ratios in aerosols at Gosan, Jeju Island: Implications for atmospheric processing and source changes of aerosols, J. Geophys. Res., 115, https://doi.org/10.1029/2009JD013323, 2010.

Lamsal, L. N., Martin, R. V., Padmanabhan, A., van Donkelaar, A., Zhang, Q., Sioris, C. E., Chance, K., Kurosu, T. P., Newchurch, M. J.: Application of satellite observations for timely updates to global anthropogenic NO_x emission inventories, Geophys. Res. Lett., 38, (5), https://doi.org/10.1029/2010GL046476, 2011.

Lance, S., Barth, M., and Carlton, A.: Multiphase chemistry: Experimental design for coordinated measurement and modeling studies of cloud processing at a mountaintop, B. Am. Meteorol. Soc., 98, ES163-ES167, https://doi.org/10.1175/bams-d-17-0015.1, 2017.

Leng, Q., Cui, J., Zhou, F., Du, K., Zhang, L., Fu, C., Liu, Y., Wang, H., Shi, G., Gao, M., Yang, F., and He, D.: Wet-only deposition of atmospheric inorganic nitrogen and associated isotopic characteristics in a typical mountain area, southwestern China, Sci. Total Environ., 616, 55-63, https://doi.org/10.1016/j.scitotenv.2017.10.240, 2017.

Levy, H., Moxim, W. J., Kasibhatla, P. S.: A global three-dimensional time-dependent lightning source of tropospheric NO_x, J. Geophys. Res., 101, 22911-22922, 1996.

Li, J., Wang, X., Chen, J., Zhu, C., Li, W., Li, C., Liu, L., Xu, C., Wen, L., Xue, L., Wang, W., Ding, A., and Herrmann, H.: Chemical composition and droplet size distribution of cloud at the summit of Mount Tai, China, Atmos. Chem. Phys., 17, 9885-9896, https://doi.org/10.5194/acp-17-9885-2017, 2017.

Li, L., Lollar, B. S., Li, H., Wortmann, U. G., and Lacrampe-Couloume, G.: Ammonium stability and nitrogen isotope fractionations for NH_3(aq)-NH_3(gas) systems at 20-70 °C and pH of 2-13: Applications to habitability and nitrogen cycling in low-temperature hydrothermal systems, Geochim. Cosmochim. Ac., 84, 280-296, https://doi.org/10.1016/j.gca.2012.01.040, 2012.

Li, Q., Jiang, J., Cai, S., Zhou, W., Wang, S., Duan, L., and Hao, J.: Gaseous ammonia emissions from coal and biomass combustion in household stoves with different combustion efficiencies, Environ. Sci. Technol. Lett., 3, 98-103, https://doi.org/10.1021/acs.estlett.6b00013, 2016a.

Li, T., Wang, Y., Mao, H., Wang, S., Talbot, R. W., Zhou, Y., Wang, Z., Nie, X., and Qie, G.: Insights on chemistry of mercury species in clouds over Northern China: Complexation and adsorption, Environ. Sci. Technol., 52, 5125-5134, https://doi.org/10.1021/acs.est.7b06669, 2018.

Li, Y., Schichtel, B. A., Walker, J. T., Schwede, D. B., Chen, X., Lehmann, C. M. B., Puchalski, M. A., Gay, D. A., and Collett, J. L.: Increasing importance of deposition of reduced nitrogen in the United States, P. Natl. Acad. Sci. USA., https://doi.org/10.1073/pnas.1525736113, 2016b.

Lin, C. T., Jickells, T. D., Baker, A. R., Marca, A., and Johnson, M. T.: Aerosol isotopic ammonium signatures over the remote Atlantic Ocean, Atmos. Environ., 133, 165-169, https://doi.org/10.1016/j.atmosenv.2016.03.020, 2016.

Lin, Q., Zhang, G., Peng, L., Bi, X., Wang, X., Brechtel, F. J., Li, M., Chen, D., Peng, P., Sheng, G., and Zhou, Z.: In situ chemical composition measurement of individual cloud residue particles at a mountain site, southern China, Atmos. Chem. Phys., 17, 8473-8488, https://doi.org/10.5194/acp-17-8473-2017, 2017.

Liu, D., Fang, Y., Tu, Y., and Pan, Y.: Chemical method for nitrogen isotopic analysis of ammonium at natural abundance, Anal. Chem., 86, 3787-3792, https://doi.org/10.1021/ac403756u, 2014.

Liu, X., Zhang, Y., Han, W., Tang, A., Shen, J., Cui, Z., Vitousek, P., Erisman, J. W., Goulding, K., Christie, P., Fangmeier, A., and Zhang, F.: Enhanced nitrogen deposition over China. Nature, 494, 459-462, https://doi.org/10.1038/nature11917, 2013.

Liu, L., Zhang, J., Xu, L., Yuan, Q., Huang, D., Chen, J., Shi, Z., Sun, Y., Fu, P., Wang, Z., Zhang, D., and Li, W.: Cloud scavenging of anthropogenic refractory particles at a mountain site in North China, Atmos. Chem. Phys., 18, 14681-14693, https://doi.org/10.5194/acp-18-14681-2018, 2018.

Lobert, J. M., Scharffe, D. H., Hao, W. M., and Crutzen, P. J.: Importance of biomass burning in the atmospheric budgets of nitrogen-containing gases. Nature, 346, 552, https://doi.org/10.1038/346552a0, 1990.

McIlvin, M. R., and Altabet, M. A.: Chemical conversion of nitrate and nitrite to nitrous oxide for nitrogen and oxygen isotopic analysis in freshwater and seawater, Anal. Chem., 77, 5589-5595, https://doi.org/10.1021/ac050528s, 2005.

Michalski, G., Bockheim, J. G., Kendall, C., and Thiemens, M.: Isotopic composition of Antarctic Dry Valley nitrate: Implications for NO_y sources and cycling in Antarctica, Geophys. Res. Lett., 32, https://doi.org/10.1029/2004GL022121, 2005.

Michalski, G., Bhattacharya, S., and Mase, F.: Oxygen isotope dynamics of atmospheric nitrate and its precursor molecules (Chapter 30), in M. Baskaran (ed.), Handbook of Environmental Isotope Geochemistry, Advances in Isotope Geochemistry, https://doi.org/10.1007/978-3-642-10637-8_30, Springer-Verlag, Berlin Heidelberg, 2011.

Miyazaki, K., Eskes, H., Sudo, K., Boersma, K. F., Bowman, K., Kanaya, Y.: Decadal changes in global surface NO_x emissions from multi-constituent satellite data assimilation, Atmos. Chem. Phys., 17, 807-837, 2017.

Morin, S., Savarino, J., Frey, M. M., Yan, N., Bekki, S., Bottenheim, J. W., and Martins, J. M.: Tracing the origin and fate of NO_x in the Arctic atmosphere using stable isotopes in nitrate. Science, 322, 730-732, https://doi.org/ 10.1126/science.1161910, 2008.

Morino, Y., Kondo, Y., Takegawa, N., Miyazaki, Y., Kita, K., Komazaki, Y., Fukuda, M., Miyakawa, T., Moteki, N., Worsnop, D. R.: Partitioning of HNO_3 and particulate nitrate over Tokyo: Effect of vertical mixing, J. Geophys. Res., 111, https://doi.org/10.1029/2005JD006887, 2006.

Norris, J. R., Allen, R. J., Evan, A. T., Zelinka, M. D., O'Dell, C. W., and Klein, S. A.: Evidence for climate change in the satellite cloud record. Nature, 536, 72, https://doi.org/10.1038/nature18273, 2016.

Okin, G. S., Baker, A. R., Tegen, I., Mahowald, N. M., Dentener, F. J., Duce, R. A., Galloway, J. N., Hunter, K., Kanakidou, M., Kubilay, N., Prospero, J. M., Sarin, M., Surapipith, V., Uematsu, M., and Zhu, T.: Impacts of atmospheric nutrient deposition on marine productivity: Roles of nitrogen, phosphorus, and iron. Global Biogeochem. Cy., 25, https://doi.org/doi:10.1029/2010GB003858, 2011.

Olivier, J., Bouwman, A., Van der Hoek, K., and Berdowski, J.: Global air emission inventories for anthropogenic sources of NO_x, NH_3 and N_2O in 1990, Environ. Pollut., 102, 135-148, https://doi.org/10.1016/B978-0-08-043201-4.50024-1, 1998.

Park, Y., Park, K., Kim, H., Yu, S., Noh, S., Kim, M., Kim, J., Ahn, J., Lee, M., Seok, K., and Kim, Y.: Characterizing isotopic compositions of TC-C, NO_3^--N, and NH_4^+-N in $PM_{2.5}$ in South Korea: Impact of China's winter heating, Environ. Pollut., 233, 735-744, https://doi.org/10.1016/j.envpol.2017.10.072, 2018.

Paulot, F. and Jacob, D. J.: Hidden cost of US agricultural exports: particulate matter from ammonia emissions, Environ. Sci. Technol., 48, 903-908, 2014.

Proemse, B. C., Mayer, B., Chow, J. C., and Watson, J. G.: Isotopic characterization of nitrate, ammonium and sulfate in stack $PM_{2.5}$ emissions in the Athabasca Oil Sands Region, Alberta, Canada, Atmos. Environ., 60, 555-563, https://doi.org/10.1016/j.atmosenv.2012.06.046, 2012.

Price, C., Penner, J., Prather, M.: NO_x from lightning: 1. Global distribution based on lightning physics, J. Geophys. Res., 102, 5929-5941, 1997.

Ravishankara, A. R.: Heterogeneous and multiphase chemistry in the troposphere. Science, 276, 1058-1065, https://doi.org/10.1126/science.276.5315.1058, 1997.

Reche, C., Viana, M., Pandolfi, M., Alastuey, A., Moreno, T., Amato, F., Ripoll, A., Querol, X.: Urban NH_3 levels and sources in a Mediterranean environment, Atmos. Environ., 57, 153-164, 2012.

Reis, S., Pinder, R. W., Zhang, M., Lijie, G., Sutton, M. A.: Reactive nitrogen in atmospheric emission inventories, Atmos. Chem. Phys., 9, 7657-7677, 2009.

Richter, A., Burrows, J. P., Nuss, H., Granier, C., Niemeier, U.: Increase in tropospheric nitrogen dioxide over China observed from space. Nature, 437, 129-132, 2005.

Sang, X. F., Gensch, I., Kammer, B., Khan, A., Kleist, E., Laumer, W., Schlag, P., Schmitt, S. H., Wildt, J., Zhao, R., Mungall, E. L., Abbatt, J. P. D., and Kiendler-Scharr, A.: Chemical stability of levoglucosan: an isotopic perspective, Geophys. Res. Lett., 43, 5419-5424, https://doi.org/10.1002/2016GL069179, 2016.

Savard, M. M., Cole, A. S., Vet, R., and Smirnoff, A.: The $\Delta^{17}O$ and $\delta^{18}O$ values of atmospheric nitrates simultaneously collected downwind of anthropogenic sources - implications for polluted air masses, Atmos. Chem. Phys., 18, 10373-10389, https://doi.org/10.5194/acp-18-10373-2018, 2018.

Seinfeld, J. and Pandis, S. N.: Atmospheric Chemistry and Physics: From air pollution to climate change. John Wiley and Sons, 2012.

Schlesinger, W., and Hartley, A.: A global budget for atmospheric NH_3. Biogeochem., 15, 191-211, https://doi.org/10.1007/BF00002936, 1992.

Schurman, M. I., Boris, A., Desyaterik, Y., and Collett, J. L.: Aqueous secondary organic aerosol formation in ambient cloud water photo-oxidations, Aerosol Air Qual. Res., 18, 15-25, https://doi.org/10.4209/aaqr.2017.01.0029, 2018.

Seinfeld, J. H., Bretherton, C., Carslaw, K. S., Coe, H., DeMott, P. J., Dunlea, E. J., Feingold, G., Ghan, S., Guenther, A. B., Kahn, R., Kraucunas, I., Kreidenweis, S. M., Molina, M. J., Nenes, A., Penner, J. E., Prather, K. A., Ramanathan, V., Ramaswamy, V., Rasch, P. J., Ravishankara, A. R., Rosenfeld, D., Stephens, G., and Wood, R.: Improving our fundamental understanding of the role of aerosol-cloud interactions in the climate system, P. Natl. Acad. Sci. USA., 113, 5781-5790, https://doi.org/10.1073/pnas.1514043113, 2016.

Slade, J. H., Shiraiwa, M., Arangio, A., Su, H., Pöschl, U., Wang, J., and Knopf, D. A.: Cloud droplet activation through oxidation of organic aerosol influenced by temperature and particle phase state, Geophys. Res. Lett., 44, 1583-1591, https://doi.org/doi:10.1002/2016GL072424, 2017.

Smirnoff, A., Savard, M. M., Vet, R., and Simard, M. C.: Nitrogen and triple oxygen isotopes in near-road air samples using chemical conversion and thermal decomposition, Rapid Commun. Mass Sp., 26, 2791-2804, https://doi.org/10.1002/rcm.6406, 2012.

Souri, A. H., Choi, Y., Jeon, W., Kochanski, A. K., Diao, L., Mandel, J., Bhave, P. V., and Pan, S.: Quantifying the impact of biomass burning emissions on major inorganic aerosols and their precursors in the U.S, J. Geophys. Res., 122, 12, https://doi.org/10.1002/2017JD026788, 2017.

Suarez-Bertoa, R., Zardini, A. A., Astorga, C.: Ammonia exhaust emissions from spark ignition vehicles over the New European Driving Cycle, Atmos. Environ., 97, 43-53, 2014.

Teng, X., Hu, Q., Zhang, L., Qi, J., Shi, J., Xie, H., Gao, H., Yao, X.: Identification of major sources of atmospheric NH_3 in an urban environment in Northern China during wintertime, Environ. Sci. Technol., 51, 6839-6848, 2017.

Tu, Y., Fang, Y., Liu, D., and Pan, Y.: Modifications to the azide method for nitrate isotope analysis, Rapid Commun. Mass Sp., 30, 1213-1222, https://doi.org/10.1002/rcm.7551, 2016.

van Pinxteren, D., Fomba, K. W., Mertes, S., Müller, K., Spindler, G., Schneider, J., Lee, T., Collett, J. L., and Herrmann, H.: Cloud water composition during HCCT-2010: Scavenging efficiencies, solute concentrations, and droplet size dependence of inorganic ions and dissolved organic carbon, Atmos. Chem. Phys., 16, 3185-3205, https://doi.org/10.5194/acp-16-3185-2016, 2016.

Vega, C., Mårtensson, M., Wideqvist, U., Kaiser, J., Zieger, P., and StrÖm, J.: Composition, isotopic fingerprint and source attribution of nitrate deposition from rain and fog at a Sub-Arctic Mountain site in Central Sweden (Mt Åreskutan), Tellus B, 71, 1445379, https://doi.org/10.1080/16000889.2018.1559398, 2019.

Voigt, A., and Shaw, T. A.: Circulation response to warming shaped by radiative changes of clouds and water vapour, Nature Geosci., 8, 102-106, https://doi.org/10.1038/ngeo2345, 2015.

Walters, W. W., Goodwin, S. R., and Michalski, G.: Nitrogen stable isotope composition ($\delta^{15}N$) of vehicle-emitted NO_x, Environ. Sci. Technol., 49, 2278-2285, https://10.1021/es505580v, 2015a.

Walters, W. W., and Michalski, G.: Theoretical calculation of nitrogen isotope equilibrium exchange fractionation factors for various NO_y molecules, Geochim. Cosmochim. Ac., 164, 284-297, https://doi.org/10.1016/j.gca.2015.05.029, 2015.

Walters, W. W., Simonini, D. S., and Michalski, G.: Nitrogen isotope exchange between NO and NO_2 and its implications for $\delta^{15}N$ variations in tropospheric NO_x and atmospheric nitrate, Geophys. Res. Lett., 43, 440-448, https://doi.org/10.1002/2015gl066438, 2016.

Walters, W. W., Tharp, B. D., Fang, H., Kozak, B. J., and Michalski, G.: Nitrogen isotope composition of thermally produced NO_x from various fossil-fuel combustion sources, Environ. Sci. Technol., 49, 11363-11371, https://doi.org/10.1021/acs.est.5b02769, 2015b.

Wang, Y. L., Liu, X. Y., Song, W., Yang, W., Han, B., Dou, X. Y., Zhao, X. D., Song, Z. L., Liu, C. Q., and Bai, Z. P.: Source appointment of nitrogen in $PM_{2.5}$ based on bulk $\delta^{15}N$ signatures and a Bayesian isotope mixing model, Tellus B, 69, 1299672, https://doi.org/10.1080/16000889.2017.1299672, 2017a.

Wang, Z., Wang, W., Tham, Y. J., Li, Q., Wang, H., Wen, L., Wang, X., Wang, T.: Fast heterogeneous N_2O_5 uptake and $ClNO_2$ production in power plant and industrial plumes observed in the nocturnal residual layer over the North China Plain, Atmos. Chem. Phys., 17, 12361-12378, 2017b.

Weathers, K. C., and Likens, G. E.: Clouds in Southern Chile: An important source of nitrogen to nitrogen-limited ecosystems?, Environ. Sci. Technol., 31, 210-213, https://doi.org/10.1021/es9603416, 1997.

Yang, J. Y. T., Hsu, S. C., Dai, M. H., Hsiao, S. S. Y., and Kao, S. J.: Isotopic composition of water-soluble nitrate in bulk atmospheric deposition at Dongsha Island: Sources and implications of external N supply to the northern South China Sea. Biogeosci., 11, 1833-1846, https://doi.org/10.5194/bg-11-1833-2014, 2014.

Yeatman, S., Spokes, L., Dennis, P., and Jickells, T.: Comparisons of aerosol nitrogen isotopic composition at two polluted coastal sites, Atmos. Environ., 35, 1307-1320, https://doi.org/10.1016/S1352-2310(00)00408-8, 2001.

Yienger, J. J. and Levy, H.: Empirical model of global soil-biogenic NO_x emissions, J. Geophys. Res., 100, 11447-11464, 1995.

Zhang, C., Geng, X., Wang, H., Zhou, L., Wang, B.: Emission factor for atmospheric ammonia from a typical municipal wastewater treatment plant in South China, Environ. Pollut., 220, 963-970, 2017.

Zhang, L., Chen, Y., Zhao, Y., Henze, D. K., Zhu, L., Song, Y., Paulot, F., Liu, X., Pan, Y., Lin, Y., Huang, B.: Agricultural ammonia emissions in China: Reconciling bottom-up and top-down estimates, Atmos. Chem. Phys., 18, 339-355, 2018.

Zhang, Y. L., and Cao, F.: Is it time to tackle $PM_{2.5}$ air pollutions in China from biomass-burning emissions?, Environ. Pollut., 202, 217-219, https://doi.org/10.1016/j.envpol.2015.02.005, 2015.

Zhang, Y., Zheng, L. X., Liu, X. J., Jickells, T., Cape, J. N., Goulding, K., Fangmeier, A., and Zhang, F. S.: Evidence for organic N deposition and its anthropogenic sources in China, Atmos. Environ., 42, 1035-1041, https://doi.org/10.1016/j.atmosenv.2007.12.015, 2008.

Zhang, Y., Dore, A. J., Ma, L., Liu, X. J., Ma, W. Q., Cape, J. N., and Zhang, F. S.: Agricultural ammonia emissions inventory and spatial distribution in the North China Plain, Environ. Pollut., 158, 490-501, https://doi.org/10.1016/j.atmosenv.2007.12.015, 2010.

Zhao, Y., Zhang, J., and Nielsen, C. P.: The effects of recent control policies on trends in emissions of anthropogenic atmospheric pollutants and CO_2 in China, Atmos. Chem. Phys., 13, 487-508, https://doi.org/10.5194/acp-13-487-2013, 2013.

Zheng, X. D., Liu, X. Y., Song, W., Sun, X. C., and Liu, C. Q.: Nitrogen isotope variations of ammonium across rain events: Implications for different scavenging between ammonia and particulate ammonium, Environ. Pollut., 239, 392-398, https://doi.org/10.1016/j.envpol.2018.04.015, 2018.

Zong, Z., Wang, X., Tian, C., Chen, Y., Fang, Y., Zhang, F., Li, C., Sun, J., Li, J., and Zhang, G.: First assessment of NO_x sources at a regional background site in North China using isotopic analysis linked with modeling, Environ. Sci. Technol., 51, https://doi.org/10.1021/acs.est.6b06316, 2017.

Reference

Felix, J. D.; Elliott, E. M.; Avery, G. B.; Kieber, R. J.; Mead, R. N.; Willey, J. D.; Mullaugh, K. M., Isotopic composition of nitrate in sequential Hurricane Irene precipitation samples: Implications for changing NO_x sources. *Atmos. Environ.* **2015,** *106*, 191-195.

Felix, J. D.; Elliott, E. M.; Shaw, S. L., Nitrogen isotopic composition of coal-fired power plant NO_x: influence of emission controls and implications for global emission inventories. *Environ. Sci. Technol.* **2012,** *46*, (6), 3528-3535.

Felix, J. D.; Elliott, E. M., Isotopic composition of passively collected nitrogen dioxide emissions: Vehicle, soil and livestock source signatures. *Atmos. Environ.* **2014,** *92*, 359-366.

Felix, J. D.; Elliott, E. M., The agricultural history of human-nitrogen interactions as recorded in ice core $\delta^{15}N\text{-}NO_3^-$. *Geophy. Res. Lett.* **2013,** *40*, (8), 1642-1646.

Fibiger, D. L.; Hastings, M. G., First measurements of the nitrogen isotopic composition of NO_x from biomass burning. *Environ. Sci. Technol.* **2016,** *50*, (21), 11569-11574.

Hastings, M. G.; Jarvis, J. C.; Steig, E. J., Anthropogenic impacts on nitrogen isotopes of ice-core nitrate. *Science* **2009,** *324*, (5932), 1288-1288.

Heaton, T. H. E.; Spiro, B.; Madeline, S.; Robertson, C., Potential canopy influences on the isotopic composition of nitrogen and sulphur in atmospheric deposition. *Oecologia* **1997,** *109*, (4), 600-607.

Walters, W. W.; Tharp, B. D.; Fang, H.; Kozak, B. J.; Michalski, G., Nitrogen isotope composition of thermally produced NO_x from various fossil-fuel combustion sources. *Environ. Sci. Technol.* **2015,** *49*, (19), 11363-11371.

Walters, W. W.; Goodwin, S. R.; Michalski, G., Nitrogen stable isotope composition (δ^{15}N) of vehicle-emitted NO_x. *Environ. Sci. Technol.* **2015,** *49*, (4), 2278-2285.

设置了格式: 字体: 小四

带格式的: 两端对齐